SUPPLEMENTAL INFORMATION

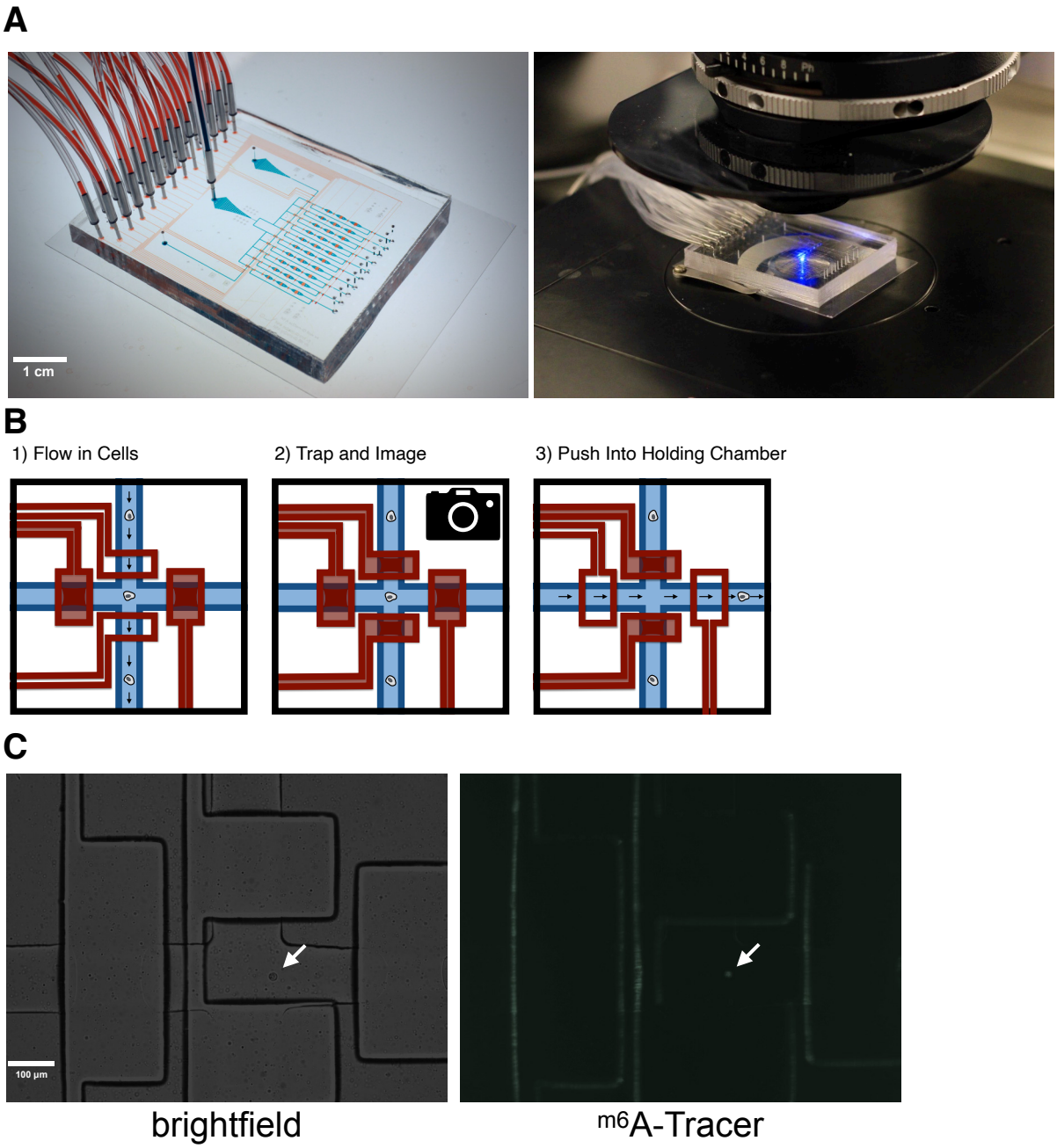

Figure S1. Illustration of cell trapping procedure, related to Figure 1.

(A) an image of the µDamID device, with the flow layer filled with blue food coloring and the control layer filled with red food coloring, alongside an image of the device as operated on an inverted microscope.

(B) Cells are driven through the device by peristaltic pumping or pressure-driven flow. Valves are actuated to confine the cell in the trapping region, where it is imaged, and if selected, it is pushed by dead-end filling into a holding chamber to the right of the trapping region.

(C) 10X magnification images of an actual cell held in the trapping chamber prior to high-resolution imaging and sequencing (cell #018, expressing untethered Dam).

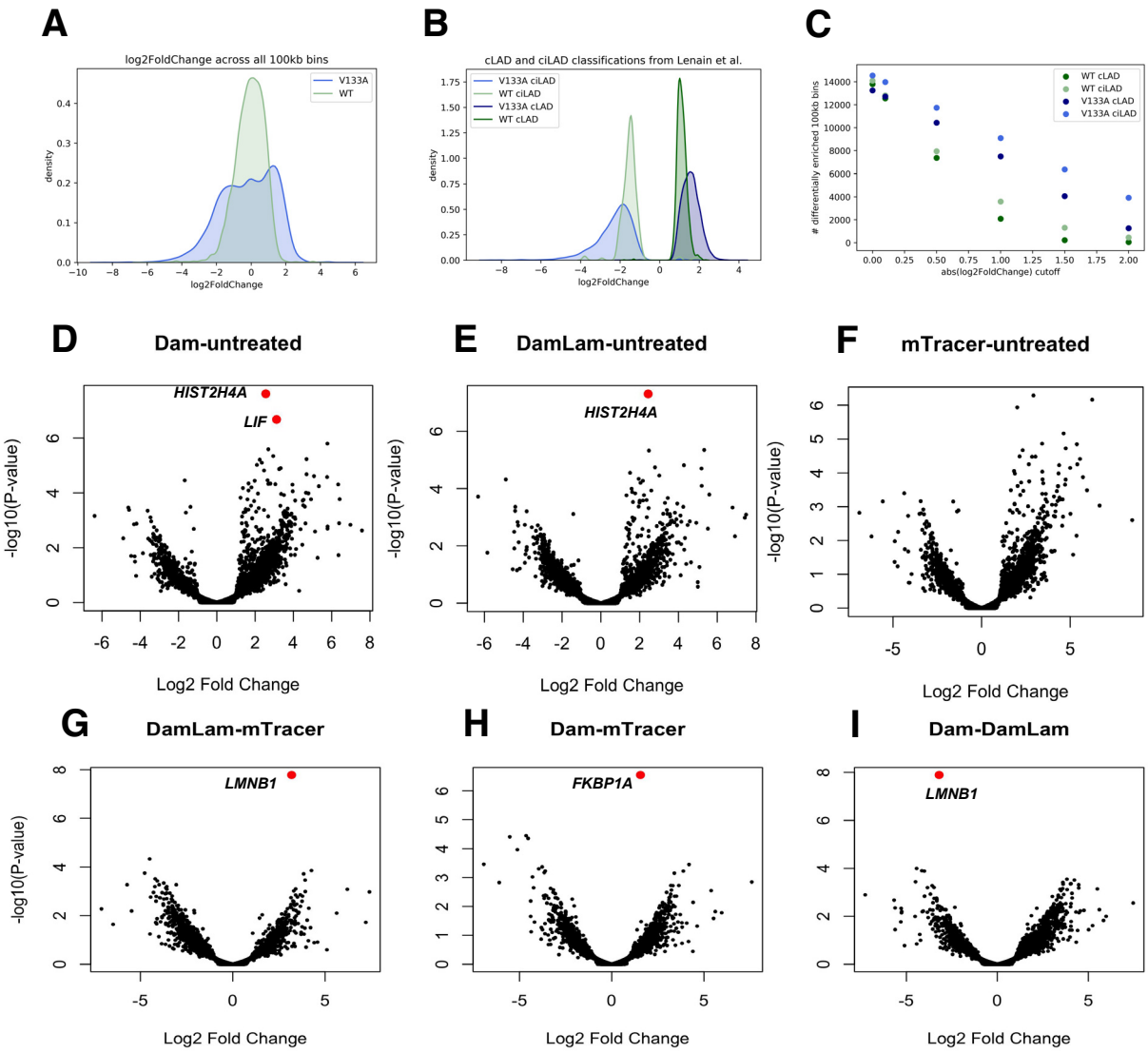

Figure S2. Comparing Dam mutants & examining effect of Dam on gene expression, related to Figure 2.

(A) Kernel density estimate of log_2FoldChange from DESeq2 differential enrichment analysis of Dam-LMNB1 coverage compared to Dam-only as reference. With V133A, more extreme log_2FoldChange values are observed with greater separation between the positive and negative log_2FoldChange peaks. In other words, compared to wild-type, the V133A Dam-LMNB1 and Dam-only signals are more distinct.

(B) Kernel density estimate of log_2 Fold Change, with cLAD/ciLAD classification from Lenain et al. 2017 indicated, shows greater separation for cLAD and ciLAD signal with V133A.

(C) V133A has higher sensitivity than WT, with more differentially enriched regions at each log_2FoldChange threshold for calling significant differential enrichment.

(D-I) Significantly differentially expressed genes (logFC significantly > 1 and adjusted p-value < 0.01) are indicated in red for bulk HEK293T cells transfected with Dam, Dam-LMNB1, ^{m6}A-Tracer, or no treatment control. Differentially expressed genes compared to no treatment control are *HIST2H4A* and *LIF* for Dam, *HIST2H4A* for Dam-LMNB1, and no genes for ^{m6}A-Tracer. When comparing Dam to ^{m6}A-Tracer, the only differentially expressed gene is *FKBP1A*, which is expected given the mutated FKBP1A-derived destabilization domain tethered to Dam in our construct. When comparing Dam-LMNB1 to ^{m6}A-Tracer, the only differentially expressed gene is *LMNB1*, which is again expected given *LMNB1* is expressed from the *Dam-LMNB1* construct itself.

A

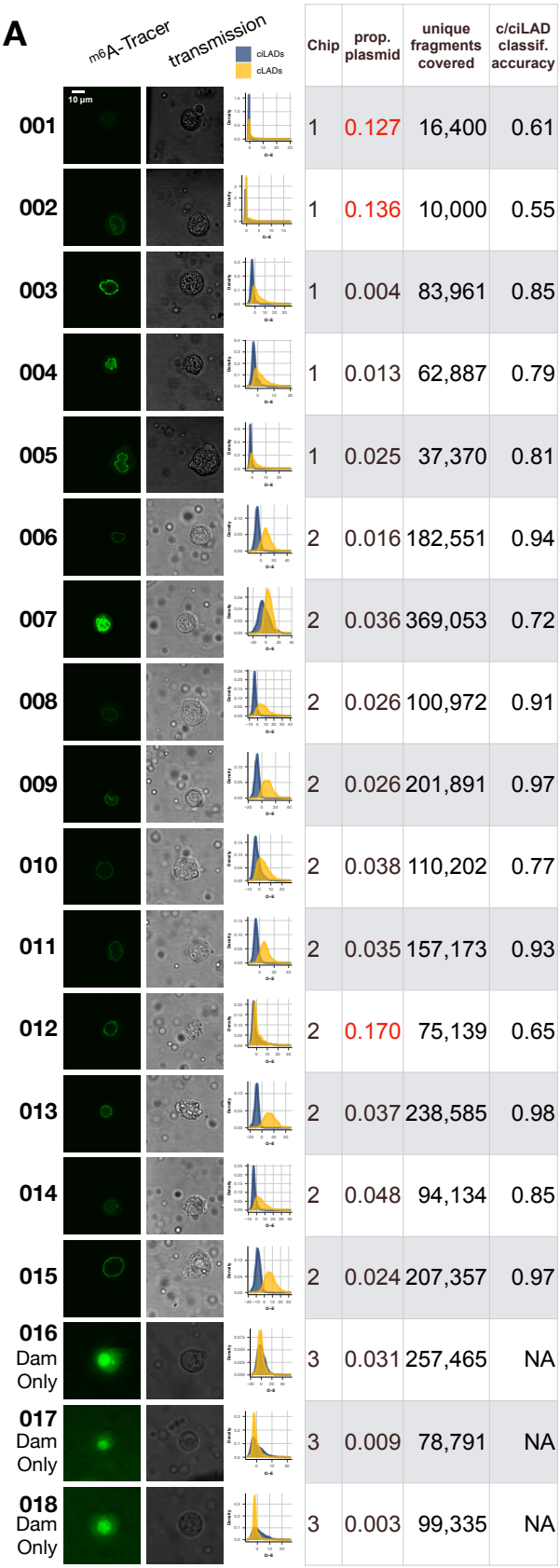

	Chip	prop. plasmid	unique fragments covered	c/ciLAD classif. accuracy
001	1	0.127	16,400	0.61
002	1	0.136	10,000	0.55
003	1	0.004	83,961	0.85
004	1	0.013	62,887	0.79
005	1	0.025	37,370	0.81
006	2	0.016	182,551	0.94
007	2	0.036	369,053	0.72
008	2	0.026	100,972	0.91
009	2	0.026	201,891	0.97
010	2	0.038	110,202	0.77
011	2	0.035	157,173	0.93
012	2	0.170	75,139	0.65
013	2	0.037	238,585	0.98
014	2	0.048	94,134	0.85
015	2	0.024	207,357	0.97
016 Dam Only	3	0.031	257,465	NA
017 Dam Only	3	0.009	78,791	NA
018 Dam Only	3	0.003	99,335	NA

Figure S3. Images and sequencing statistics for each cell, related to Figure 2.

(A) Each row corresponds to a single batch 1 cell, showing its ^{m6}A-Tracer image, transmission image, coverage distributions in c/ciLAD control regions, identifier for the device (chip) it was sequenced on, proportion of reads mapping to the transfected plasmid, number of unique DpnI fragments covered in the genome, and classification accuracy on the c/ciLAD control regions. Nine confocal ^{m6}A-Tracer images from unsequenced Dam-only cells are provided for comparison to the widefield images acquired for cells 015, 016, and 018.

(B) Next Page: as in (A) but for 40 batch 2 cells, with Dam-tdTomato-LMNB1 images and library DNA yields added. Letters in each cell identifier indicate which device they were processed on.

confocal images of 9 additional Dam-only cells (not sequenced)

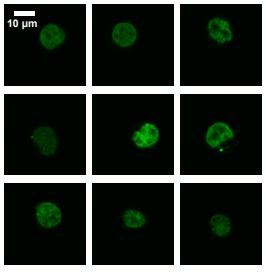

B

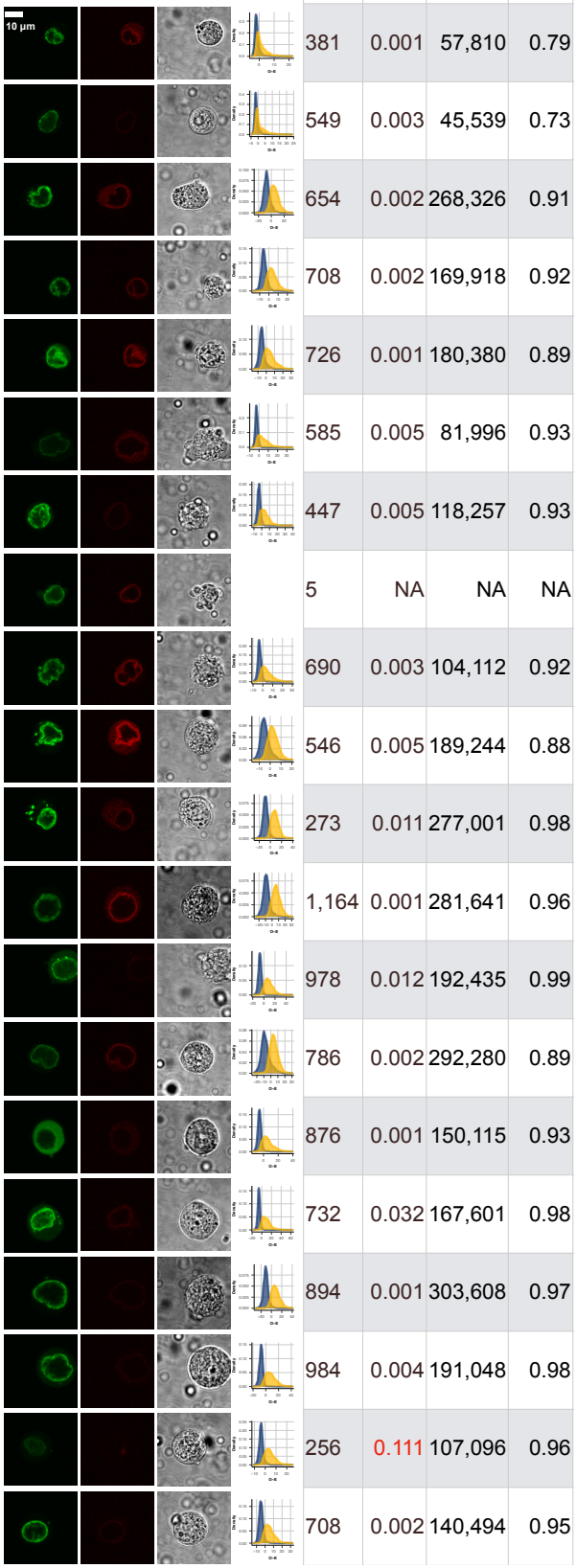

	DNA yield (ng)	prop. plasmid	unique fragments covered	c/ciLAD classif. accuracy
A01	381	0.001	57,810	0.79
A02	549	0.003	45,539	0.73
A03	654	0.002	268,326	0.91
A04	708	0.002	169,918	0.92
A05	726	0.001	180,380	0.89
A06	585	0.005	81,996	0.93
A07	447	0.005	118,257	0.93
A08	5	NA	NA	NA
A09	690	0.003	104,112	0.92
A10	546	0.005	189,244	0.88
B01	273	0.011	277,001	0.98
B02	1,164	0.001	281,641	0.96
B03	978	0.012	192,435	0.99
B04	786	0.002	292,280	0.89
B05	876	0.001	150,115	0.93
B06	732	0.032	167,601	0.98
B07	894	0.001	303,608	0.97
B08	984	0.004	191,048	0.98
B09	256	0.111	107,096	0.96
B10	708	0.002	140,494	0.95

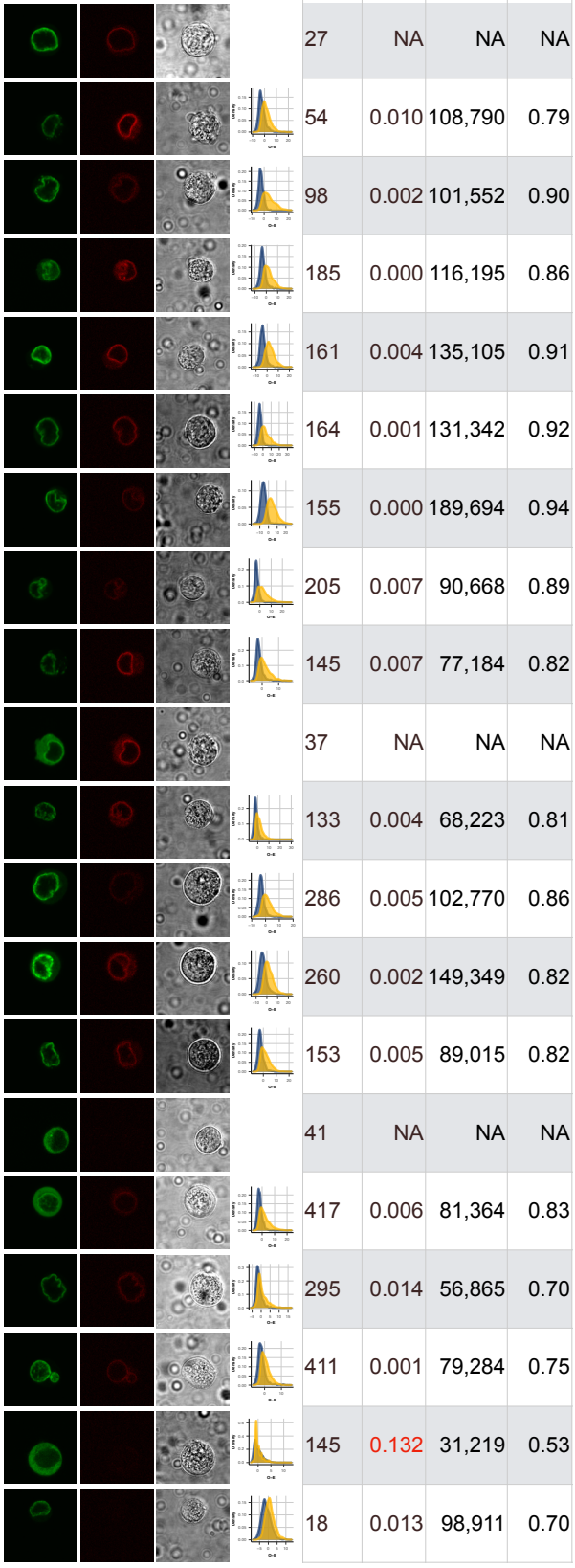

	DNA yield (ng)	prop. plasmid	unique fragments covered	c/ciLAD classif. accuracy
C01	27	NA	NA	NA
C02	54	0.010	108,790	0.79
C03	98	0.002	101,552	0.90
C04	185	0.000	116,195	0.86
C05	161	0.004	135,105	0.91
C06	164	0.001	131,342	0.92
C07	155	0.000	189,694	0.94
C08	205	0.007	90,668	0.89
C09	145	0.007	77,184	0.82
C10	37	NA	NA	NA
D01	133	0.004	68,223	0.81
D02	286	0.005	102,770	0.86
D03	260	0.002	149,349	0.82
D04	153	0.005	89,015	0.82
D05	41	NA	NA	NA
D06	417	0.006	81,364	0.83
D07	295	0.014	56,865	0.70
D08	411	0.001	79,284	0.75
D09	145	0.132	31,219	0.53
D10	18	0.013	98,911	0.70

Figure S3 continued

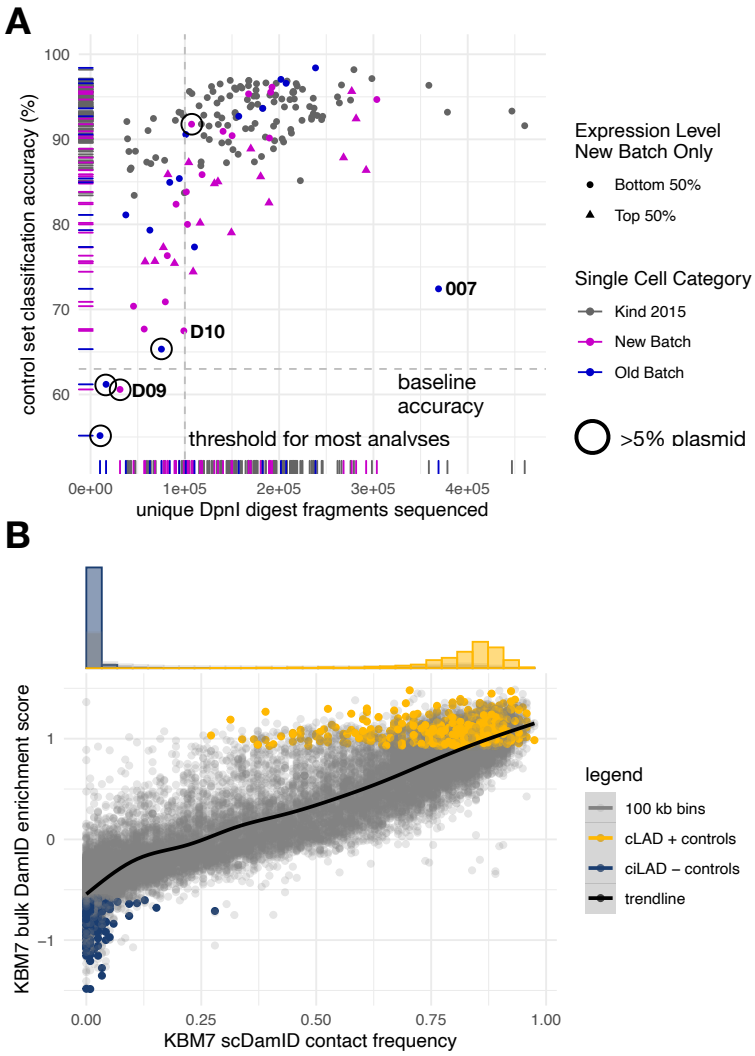

Figure S4, related to Figure 2.

(A) Similar to Figure 2D, a plot of classification accuracy vs library complexity (number of unique DpnI fragments covered), for all cells compared to single KBM7 cells from Kind et al. 2015 (gray points). Cell colors indicate which batch the cells were sequenced in, and batch 2 cells in the top half of Dam-tdTomato-LMNB1 expression levels are indicated as triangles. High-expression cells tend to have lower classification accuracies, as expected. Cells with fewer than 100k unique fragments show a drop in classification accuracy and were excluded from most downstream analyses. Cells with unusually high proportions of reads mapping to the transfection plasmid are circled. Rug plots are drawn on each axis. Cells D09 (no fluorescence at lamina or nuclear interior) and D10 (low DNA yield) are labeled, along with cell 007 (high m6A-Tracer signal in the nuclear interior, shown in Figure 3B).

(B) A plot of contact frequency vs. bulk DamID signal using data from KBM7 cells alone (Kind et al. 2015 and Lenain et al. 2017), showing high correlation (r=0.94). Sets of stringent cLADs (gold points) and ciLADs (blue points) were identified in a similar fashion to those in HEK293T cells (top 1200 by ranked bulk DamID enrichment scores, but without a p-value cutoff since none was available, which may explain larger variance in CF values). Above is a histogram showing the distribution of contact frequencies within these control sets.

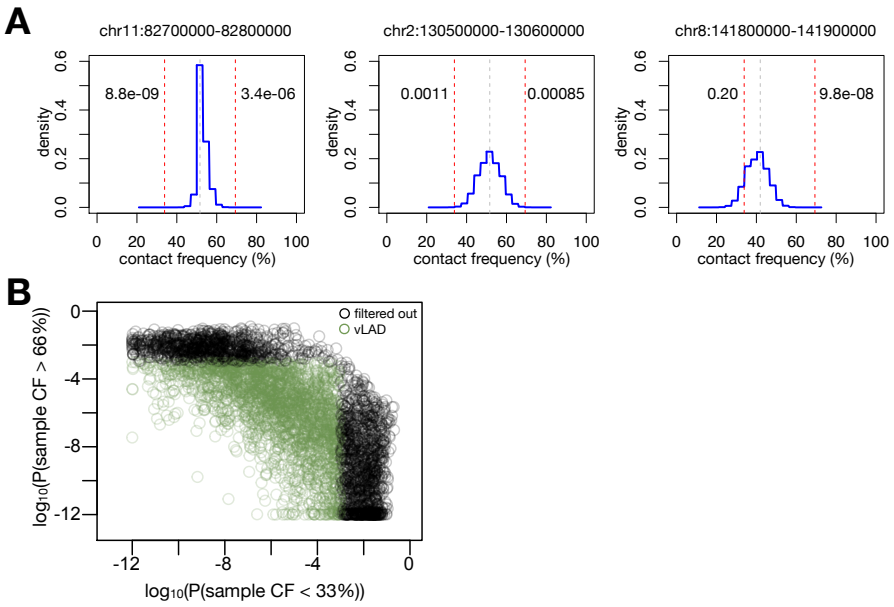

Figure S5. Modeling and comparing single-cell contact frequencies between cell types, related to Figure 4.

(A) For 3 individual bins in the genome (coordinates listed above each plot), a Poisson-Binomial distribution representing uncertainty in its sample contact frequency estimate after accounting for noise in the sequencing data (classification error rates on the control regions). Gray vertical dotted lines are the point estimate for each bin, and red dotted vertical lines are drawn at 11 and 21 out of 31 cells (CF roughly 33%-66%). Estimated probabilities of lying above or below this interval are indicated on each side of the plot. Note the difference in uncertainty between bins, as well as the difference in probabilities of lying outside the intermediate contact frequency interval.

(B) When filtering intermediate-contact-frequency bins to choose a final set of high-confidence variable LADs (vLADs), the measurement error distributions were used to select bins with the smallest probabilities of lying above or below the 33-66% CF interval ($p<0.001$ for each test, plotted in green).

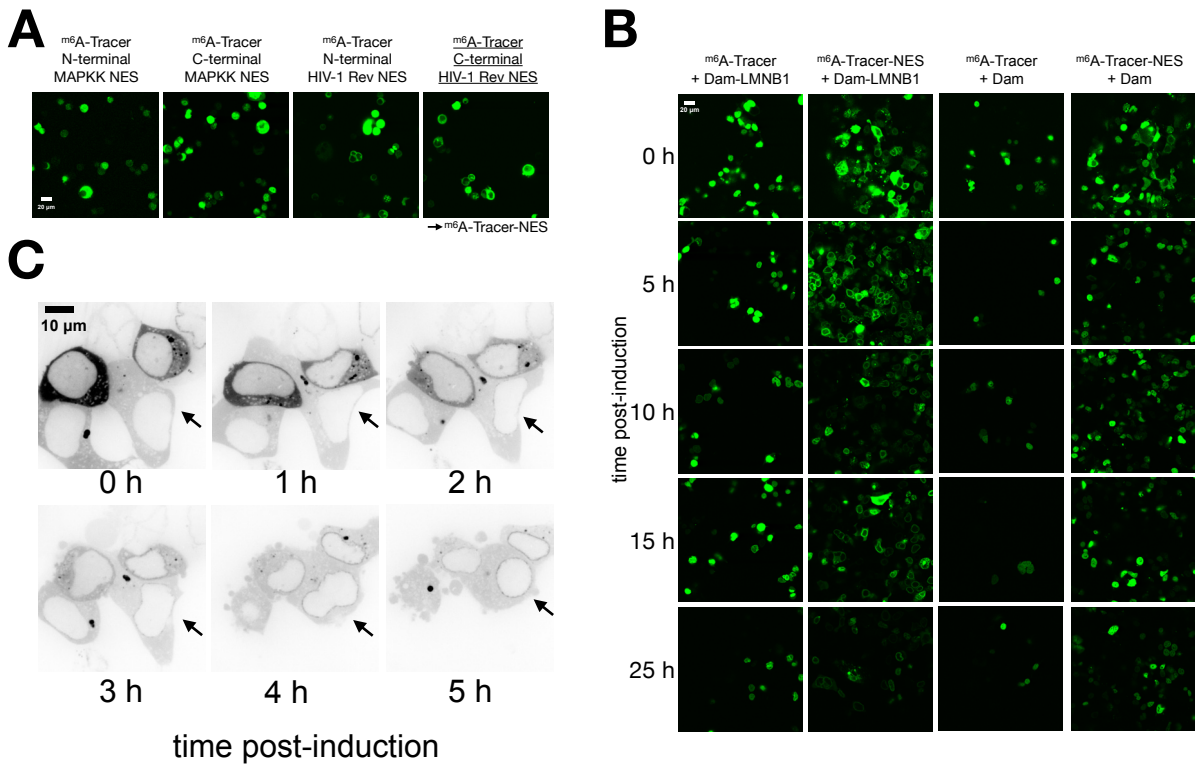

Figure S6. Additional characterization of m6A-Tracer-NES constructs, related to Figure 6.

(A) Confocal microscope images showing the localization of m6A-Tracer fluorescence when fused to one of two different Nuclear Export Signals on either terminus, in cells not expressing Dam. The HIV-1 Rev NES worked on either terminus and the C-terminal fusion was selected for downstream experiments.

(B) Time-lapse confocal images of m6A-Tracer-NES or unmodified m6A-Tracer fluorescence in different fields of cells, in cells co-expressing either Dam or Dam-LMNB1. Some nuclear localization is visible at time 0 in m6A-Tracer-NES + Dam cells, likely owing to leaky expression prior to induction.

(C) Time-lapse confocal microscope images of m6A-Tracer-NES fluorescence in the same field of cells at timepoints after Dam-LMNB1 expression. An inverted lookup table is used, and an arrow points to the nucleus of the same cell, which begins to show laminar signal around 2h post-induction.

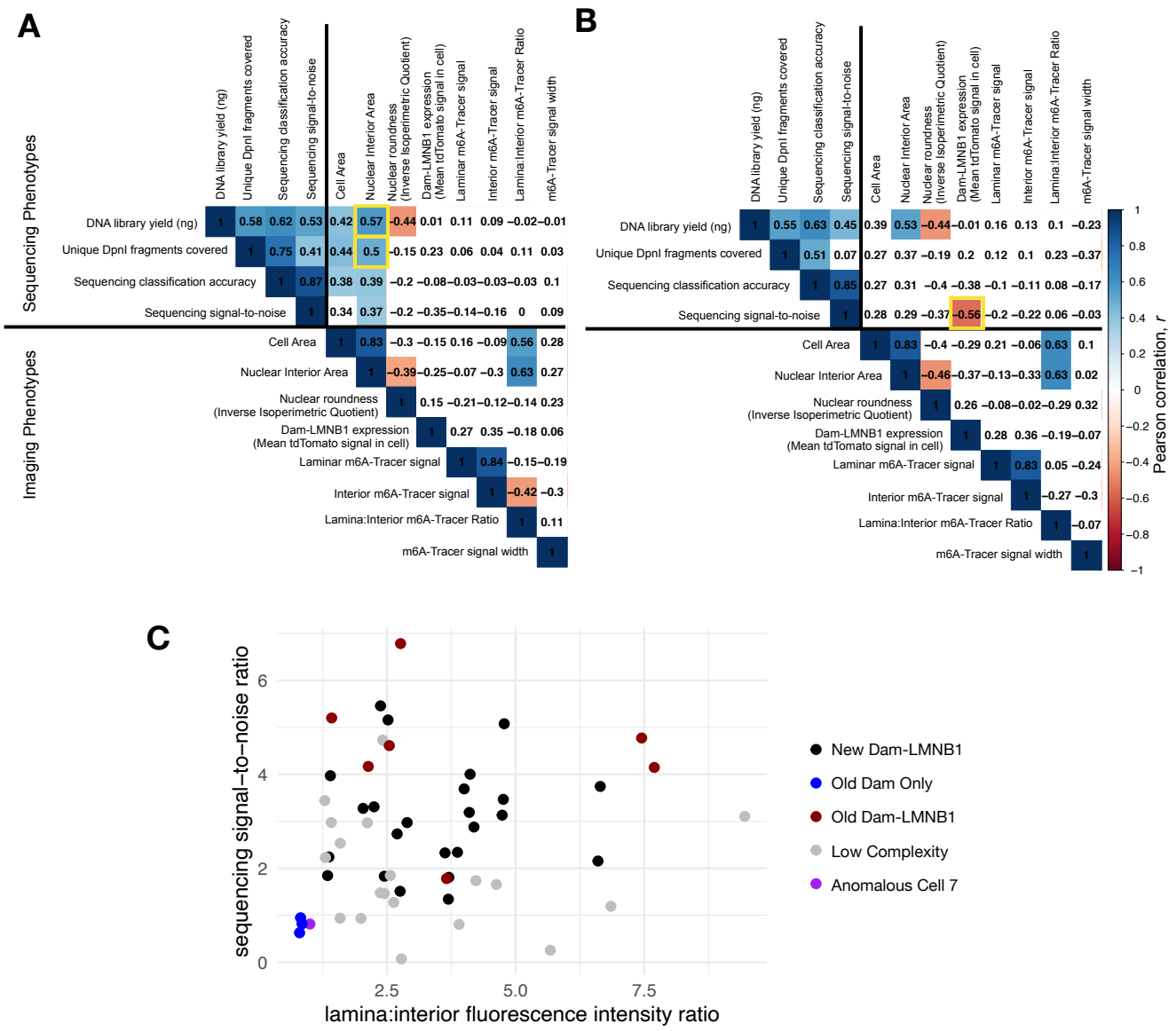

Figure S7. Correlations of sequencing and imaging phenotypes, related to Figure 7.

(A) A correlation matrix showing the relationships between imaging measures (see STAR Methods) and sequencing measures for 30 batch 2 cells with nuclear areas definable by tdTomato imaging. Correlations with p<0.05 are shaded white, while significant correlations are colored by the strength of their positive (blue) or negative (red) correlation. Associations that were further explored in Figure 7 are highlighted in yellow.

(B) As in (A) but after filtering cells to remove those with <100k unique fragments, which confound estimates of classification accuracy.

(C) Imaging ratios are reported for each cell as in Figure 3C. Dark blue points represent Dam-only cells, and dark red points and black points represent Dam-LMNB1 cells from batch 1 and batch 2, respectively. The anomalous Dam-LMNB1 cell #007 (shown in Figure 3B) is highlighted in purple. Cells with fewer than 100k unique fragments are grayed out.